Calibrating Volatility Function Bounds for An Uncertain Volatility Model* (This version: December 13, 2006)

Thomas F. Coleman † Changhong He ‡ Yuying Li §

Abstract

It is widely acknowledged that the Black-Scholes constant volatility model is inadequate in modeling underlying asset prices evidenced by the observed volatility smile. Based on the relative-entropy minimization method in Avellaneda, Friedman, Holemes & Samperi (1997), we propose a method to calibrate, from market bids and asks, a pair of volatility functions for an uncertain volatility model. The mid-prices are used to ensure separation of the lower and upper volatility functions. We show that the calibrated uncertain volatility model produces more realistic bid and ask prices, when compared with prices obtained from an uncertain volatility model with constant volatility bounds set to extreme market implied volatilities.

1 Introduction

In the classical Black-Scholes framework, a contingent claim can be replicated by the continuously trading of the primitive underlying asset. The fair value of a derivative contract is then uniquely determined based on no arbitrage pricing. This valuation methodology is preference free. Unfortunately, in the real world, markets are typically incomplete, possibly due to the existence of additional risks, e.g., volatility risk, which cannot be eliminated through trading of the underlying asset. In addition, the market provides bid and ask price pairs instead of a single price for an option.

Incomplete risk models such as stochastic volatility and jump models have been proposed for option pricing, see, e.g., Andersen & Brotherton-Ratcliffe (1998), Bakshi, Cao & Chen (1997), Duffie, Pan & Singleton (2000), Heston (1993), Hull & White (1987), Merton (1976). These models have emerged based on empirical evidence of price jumps and

*This research was also partially supported by University of Waterloo startup grants. In addition, it was conducted using resources of the Cornell Theory Center, which is supported in part by Cornell University, New York State, and members of the Corporate Partnership Program.

†Combinatorics and Optimization, University of Waterloo, 200 University Avenue West, Waterloo, Ontario, Canada N2L 3G1, email: tfcoleman@uwaterloo.ca

‡J.P. Morgan Securities Inc., 270 Park Ave, Floor 6, New York, NY, 10017-2070, email: changhong.he@jpmchase.com. Please send correspondence to this author.

§David R. Cheriton School of Computer Science, University of Waterloo, 200 University Avenue West, Waterloo, Ontario, Canada N2L 3G1, email: yuying@uwaterloo.ca

stochastic volatilities, in addition to the need to fit the volatility smile observed from option markets. However, these pricing models typically assume a representative agent maximizing a utility function and a single model price is produced for each option. Geman & Madan (2004) argue that valid solutions to market incompleteness need to be based on the practice of investment and risk management. In particular, valuation based on a representative agent with a specific utility function is not the route traders in major houses adopt when quoting prices for contingent claims which do not have a replicating portfolio. In addition, there is a practical problem concerning calibration of such a model: market option prices are not directly observable. The bid-ask midpoints are typically used as option prices. However, empirical study suggests that there is an asymmetry in option price with respect to bid-ask spreads; using bid-ask midpoints to determine a pricing model can result in a bias Nordén (2003).

In this paper, we assume that the market is incomplete due to volatility uncertainty. An uncertain volatility model (UVM) has been proposed by Avellaneda et al Avellaneda, Levy & Paras (1995); it is an incomplete market pricing model yielding a pair of price bounds. Specifically, an uncertain volatility model proposed in Avellaneda et al. (1995) assumes that, the underlying process belongs to a set of stochastic processes,

$$\begin{aligned} & \frac{dS_t}{S_t} = (r-q)dt + \sigma_t dZ_t^{\mathbb{Q}}, \\ \text{where} \quad & \underline{\sigma} \leq \sigma_t \leq \overline{\sigma}. \end{aligned} \tag{1}$$

where $\mathbb{Q}$ is a risk neutral probability measure, $Z_t^{\mathbb{Q}}$ is a standard Brownian motion under $\mathbb{Q}$, r and q are interest rate and dividend yield respectively. In addition, σ_t is non-anticipative and $\underline{\sigma}, \overline{\sigma} > 0$ are volatility bounds, which can be deterministic functions of the underlying price S and time t. Under this model, the market is incomplete due to volatility uncertainty and it is not possible to obtain a unique value for a derivative contract. Instead, an interval of no arbitrage values can be determined for each option. Such price intervals are of immediate practical use. For example, price bounds can be readily interpreted in practice as bid and ask prices.

Under an uncertain volatility model (1), the *Black-Scholes-Barenblatt* (BSB) nonlinear partial differential equation yields two bounds $\underline{V}$ and $\overline{V}$ for each option. The nonlinearity arises from the volatility that is dynamically selected according to the convexity of the option value function. For a standard European call or put, it can be shown that the upper value $\overline{V}$ is the Black-Scholes option price computed with volatility $\overline{\sigma}$ while the lower value $\underline{V}$ is the Black-Scholes option price computed with $\underline{\sigma}$. Values $\underline{V}$ and $\overline{V}$ can naturally be interpreted as bid and ask prices of the option respectively.

The main focus of this paper is to address the problem of how to calibrate an uncertain volatility model (1) for option pricing and risk management. A simple choice for an uncertain volatility model (1) is a constant volatility interval Avellaneda et al., (1995, 1996). In order for an uncertain volatility model (1) to be useful for pricing and hedging purposes, it is typically required that the model be consistent with the current liquid options prices. Unfortunately the choice of a constant volatility interval is unlikely to be consistent with all liquid market bid and ask prices. Moreover, pricing under a seemingly reasonable constant volatility interval model (1) usually leads to unreasonably large bid-ask spreads. Consider the S&P500 index options for example. As a natural candidate, let $\underline{\sigma}$ and $\overline{\sigma}$ be the minimum and maximum implied volatilities corresponding to market bid-ask mid-prices. Empirical evidence suggests that the implied volatilities for options on the same underlying and with the same maturity decrease as the strikes increase, generating volatility skew, see, e.g., Rubinstein (1994). For each option, the upper value $\overline{V}$ and lower value $\underline{V}$ are Black-Scholes prices with $\overline{\sigma}$ and $\underline{\sigma}$ respectively, since a European option value function has positive vega. Under an uncertain volatility model (1) with constant volatility bounds set to extreme implied volatilities, the difference between these two extreme option values is typically larger than the spread observed from the market. Indeed, an uncertain volatility model with constant volatility bounds implies that the implied volatilities corresponding to bids (asks) of standard options are constant, which deviates the empirical evidence. This shows that it is typically unlikely for an uncertain volatility model with constant volatility interval to be consistent with market bid and ask prices.

Calibrating a model for the underlying price based on the traded market option prices has been a standard approach for pricing and hedging options, see, e.g., Andersen & Brotherton-Ratcliffe (1998), Avellaneda et al. (1997), Coleman, Li & Verma (1999), Derman, Kani & Zou (1996), Dupire (1994), Jackson, Süli & Howison (1999), Rubinstein (1994). In the current literature, these calibration methods are typically based on either a complete market assumption or a representative agent equilibrium pricing. Under either case, there is a unique price for any given option.

In the spirit of calibrating a model from market prices, it is reasonable to consider market bid and ask prices containing information on an uncertain volatility model (1). In this paper we consider the problem of inverting the volatility bounds for an uncertain volatility model (1) from the market bid and ask prices. Availability of such a calibrated volatility uncertainty model naturally yields model bid and ask prices of other complex options and risk management methods.

Unfortunately, calibrating a pricing model from the market option prices is a challenging problem. Compared to calibration of a single volatility function in the traditional case, two volatilities $\underline{\sigma}$ and $\overline{\sigma}$, satisfying the constraint $\underline{\sigma} \leq \overline{\sigma}$, need to be determined. Moreover, there is in general *information incompleteness* when calibrating a model using only the current traded option prices. Specifically, prices are only available for a small restricted set of strikes and times to maturity. In other words, the market derivative prices provide incomplete information on an uncertain volatility model for the underlying.

Information incompleteness challenges exist even when calibrating a single risk adjusted measure, e.g., in a local deterministic volatility function model. The estimation problem typically has multiple solutions and thus is ill-posed. Various regularization methods have been considered to overcome option price incompleteness. Andersen & Brotherton-Ratcliffe (1998), Derman & Kani (1994), and Rubinstein (1994) use interpolation and extrapolation techniques to estimate missing option prices and then invert the volatility function under a finite difference method. This method is potentially problematic because interpolation, and particularly extrapolation, may introduce erroneous information. Dumas, Fleming & Whaley (1998) assume a parametric volatility function, e.g., a polynomial local volatility function. The resulting estimation problem can be well-posed but different parametric functions lead to different option prices. Coleman, Kim, Li & Verma, (1999, 2001) incorporate a smooth condition and calibrate a spline volatility function by solving a nonlinear optimization problem . Although a spline with a minimum number of knots are recommended to ensure parsimony, the selection on the number of spline knots and their placement remains challenging. Avellaneda et al. (1997) calibrate the local volatility function by minimizing relative entropy to a given prior probability measure; the prior probability can significantly affects the estimation on the volatility. In Hamida & Cont (2005), a genetic algorithm is considered to estimate different volatility functions which calibrates to market prices.

When calibrating an uncertain volatility model (1) from traded option bids and asks, incompleteness of the price information is naturally a source of volatility uncertainty. Calibrating the lower and upper volatility by interpolating or extrapolating market information seems to be inconsistent with the uncertain volatility modeling methodology. Instead, it appears more reasonable to determine a volatility uncertainty model to ensure that it is minimally biased with respect to missing information but is consistent with the current traded market bid and ask prices. Such a model naturally leads to price intervals consistent with traders' approach for quoting price intervals when the market is incomplete due to volatility uncertainty.

To calibrate a minimally biased uncertain volatility model, we use the concept of entropy, developed in information theory, as a measure of uncertainty. The maximum entropy principle states that the uniform distribution is the most unbiased distribution to the unknowns and maximizes uncertainty if no information is given. If only partial information is known, the distribution with the maximum entropy has the least prejudice to the unknowns. The relative entropy or *Kullback Leibler distance* is a measure of distance between two probability measures, see, e.g., Buchen & Kelly (1996), Cover & Thomas (1991). Given a prior probability measure, the minimum relative entropy principle states that the posterior probability measure, which is least biased to the unknowns, reaches the minimum relative entropy.

Each option price contains useful information in determining pricing measure on a probability space $(\Omega, \mathcal{F})$. For example, if option prices across all strikes and maturities are obtainable in a deterministic volatility function model, we have full information of the market and can uniquely determine the probability measure. If only limited option prices are available, the minimum relative entropy principle can be applied to estimate a probability measure which is unbiased to missing information, see, e.g., Buchen & Kelly (1996), Feittelli (2000), Rouge & Karoui (2000).

We apply the minimum relative entropy principle to calibrate the upper and lower volatility bounds for an UVM that are consistent with the market bid and ask prices. One of the objectives is for the calibrated model to be unbiased towards missing information. The volatility bounds in UVM are assumed to be deterministic functions of underlying prices and time. Suppose that the priors for both the upper and lower volatility functions are given. The extreme implied volatilities of historical ask and bid prices, for example, can be used as the priors for the upper and the lower volatilities respectively. Alternatively, priors for the upper and lower volatilities can simply be set to the extreme implied volatilities of the current bid and ask prices of different strikes and maturities.

Using the assumed priors, similar to Avellaneda et al. (1997), the upper and lower volatility functions can be determined by solving equivalent constrained optimal control problems. Unfortunately there is an additional challenge when calibrating a volatility uncertain model from market bid and ask pairs. In particular, one needs to ensure that the calibrated upper volatility $\overline{\sigma}$ is always no less than the calibrated lower volatility $\underline{\sigma}$. Note that implementation of entropy minimization also requires additional bounds on each volatility calibration respectively, see, e.g., Avellaneda et al. (1997). We use this technical constraint to satisfy the requirement that $\underline{\sigma} \leq \overline{\sigma}$. This technical constraint is implemented using a local volatility function σ_{mid} which calibrates the middle prices of bid-ask pairs.

Two computational approaches are investigated in this paper to solve the constrained optimization problem arising from the entropy minimization for calibration. One is the Lagrangian multiplier method and the other is the quadratic penalty function method. When the bid-ask spreads are small, the Lagrangian multiplier method is likely to fail to provide a solution since computational errors can lead to numerical infeasibility. The penalty function formulation, on the other hand, always yields a solution.

After an uncertain volatility model is calibrated from given bid and ask prices, we can apply it to compute bids and asks of vanilla options as well as exotic options.

The paper is organized as follows. In section 2, we first briefly review option pricing under an uncertain volatility model. We then propose mathematical formulations for calibrating volatility bounds in an uncertain volatility model based on the entropy method. In section 3 we discuss the Lagrangian formulation for the entropy optimization problem and its numerical difficulties. To overcome this difficulty, a quadratic penalty function method is proposed in section 4 to approximate a solution to the entropy optimization problem. In section 5, we illustrate the uncertain volatility intervals calibrated from bid and ask prices. In one example, bid and ask prices are generated from a constant elasticity of variance model. In the second example, S&P 500 market bid and ask prices are used. Numerical investigation shows that the calibrated uncertain volatility model yields smaller and more realistic price spreads, compared with an uncertain volatility model with constant volatility bounds from extreme implied volatilities.

2 Mathematical Formulations

Consider a set of probability spaces $\{(\Omega, \mathcal{F}, \mathbb{Q}),\ \mathbb{Q} \in \Theta\}$. Assume that the set of pricing measure Θ is specified by an uncertain volatility model (1),

$$\begin{aligned} \frac{dS_t}{S_t} &= (r-q)dt + \sigma_t dZ_t^{\mathbb{Q}}, \\ \text{where} \qquad & \underline{\sigma} \leq \sigma_t \leq \overline{\sigma} \end{aligned} \tag{2}$$

where r is the risk-free interest rate, q is the dividend rate, $Z_t^{\mathbb{Q}}$ is a standard Brownian motion under probability measure $\mathbb{Q}$, σ_t is a progressively measurable stochastic process bounded by the interval $[\underline{\sigma}, \bar{\sigma}]$. In general, the bounds $\underline{\sigma}$ and $\bar{\sigma}$ can depend on the underlying price S and time t.

Consider a European option with the payoff function $G(S)$ at the expiry T. Under an assumed uncertain volatility model (1) with fixed bounds $\underline{\sigma}$ and $\bar{\sigma}$, there are a pair of option values V^+ and V^-, $V^- \leq V^+$, associated with this option. Specifically, the pair of option values are respectively,

$$V^+(S_t, t) = \sup_{\mathbb{Q} \in \Theta} E_t^{\mathbb{Q}}[e^{-r(T-t)}G(S_T)] \tag{3}$$

and

$$V^-(S_t,t) = \inf_{\mathbb{Q}\in\Theta} E_t^{\mathbb{Q}}[e^{-r(T-t)}G(S_T)] \tag{4}$$

Based on stochastic control theory, see, e.g.,Fleming & Soner (1993), these extreme values can be computed by solving Hamilton-Jacobi-Bellman (HJB) equations. For example V^- satisfies the HJB equation below

$$-\frac{\partial V}{\partial t} + rV + \sup_{\underline{\sigma}\le\sigma\le\bar{\sigma}} \left(-(r-q)S\frac{\partial V}{\partial S} - \frac{1}{2}\sigma^2 S^2 \frac{\partial^2 V}{\partial S^2} \right) = 0.$$

These HJB equations lead to the *Black-Scholes-Barenblatt* (BSB) equation (5) below

$$\frac{\partial V}{\partial t} + (r-q)S\frac{\partial V}{\partial S} + \frac{1}{2}\left(\sigma\left[\frac{\partial^2 V}{\partial S^2}\right]\right)^2 S^2\frac{\partial^2 V}{\partial S^2} - rV = 0 \tag{5}$$

with the final condition

$$V(S,T) = G(S)$$

where V^+ is obtained with $\sigma\Big[\cdot\Big] = \sigma^+\Big[\cdot\Big]$ below

$$\sigma^+\left[\frac{\partial^2 V}{\partial S^2}\right] \stackrel{\text{def}}{=} \begin{cases} \bar{\sigma} & \text{if } \frac{\partial^2 V}{\partial S^2} \ge 0, \\ \underline{\sigma} & \text{if } \frac{\partial^2 V}{\partial S^2} < 0 \end{cases} \tag{6}$$

and V^- is obtained with $\sigma\Big[\cdot\Big] = \sigma^-\Big[\cdot\Big]$ below

$$\sigma^-\left[\frac{\partial^2 V}{\partial S^2}\right] \stackrel{\text{def}}{=} \begin{cases} \bar{\sigma} & \text{if } \frac{\partial^2 V}{\partial S^2} \le 0, \\ \underline{\sigma} & \text{if } \frac{\partial^2 V}{\partial S^2} > 0. \end{cases} \tag{7}$$

For more details, we refer the reader to Avellaneda et al. (1995).

Note that, for an uncertain volatility model (1) with constant bounds $\underline{\sigma}$ and $\bar{\sigma}$, the corresponding value bounds V^- and V^+ for standard European options are simply the values computed from the Black-Scholes formula with constant volatility $\underline{\sigma}$ and $\bar{\sigma}$ respectively. This is due to the fact that the value function from the Black-Scholes formula is convex and satisfies the BSB equation (5) with (7) for the lower bound V^- (and equation (5) with (6) for the upper bound V^+). Thus the BSB equation is reduced to the standard Black-Scholes equation when we price the extreme values for standard calls and puts.

Assume that the current cross sectional bid prices $\underline{V}$ and ask prices $\overline{V}$ are given for all strikes and maturities. We can assume that the market are excluding bid prices less than $\underline{V}$ and ask prices greater than $\overline{V}$. Thus one might imagine determining $\underline{\sigma}$ from $\underline{V}$ prices and $\overline{\sigma}$ from $\overline{V}$ prices for a UVM (1). Unfortunately, in practice bid and ask prices are available only for a limited number of strikes and maturities. It is reasonable to wonder how much information about volatility can be inferred, with minimal bias, from a set of the market bid and ask prices. In addition, what is the appropriate mathematical formulation for calibrating an uncertainty volatility model (1) from market option bids and asks?

One might also consider, for simplicity, using an uncertain volatility model with constant volatility bounds corresponding to the current extreme implied volatilities. However, this may lead to unreasonably large price intervals for liquid options and unrealistically small price intervals for highly illiquid options. In addition, determining a lower bound $\underline{\sigma}$ by calibrating to interpolated bid prices is not consistent with an uncertain volatility model.

To calibrate an uncertain volatility model using the current market price information, it is more reasonable to seek a model that is least biased with respect to the missing information. To achieve this, the relative entropy, or Kullback Leibler distance, can be used. The Kullback Leibler distance measures the difference between two probability measures, Given two probability measures $\mathbb{Q}_1$ and $\mathbb{Q}_0$, the relative entropy between $\mathbb{Q}_1$ and $\mathbb{Q}_0$ is defined as

$$\varepsilon(\mathbb{Q}_1, \mathbb{Q}_0) = \int_\Omega ln\left(\frac{d\mathbb{Q}_1}{d\mathbb{Q}_0}\right) d\mathbb{Q}_1, \tag{8}$$

where $d\mathbb{Q}_1/d\mathbb{Q}_0$ is the Radon-Nikondym derivative. In addition, the probability measure $\mathbb{Q}_1$, which minimizes the relative entropy, is the least biased towards the missing information, see, e.g., Cover & Thomas (1991).

Avellaneda et al. (1997) proposed an entropy method for choosing a single volatility function in a local deterministic volatility function model from a set of option prices. Suppose that current prices of M European options, $\{C_i\}_{i=1}^M$, are given; these prices correspond to the payoff functions $\{G_i(S)\}_{i=1}^M$ respectively. Given a prior probability measure $\mathbb{Q}_0$, the probability measure which is closest to the prior, consistent with the given prices, and which is unbiased to un-traded option prices can be determined by solving the optimization problem:

$$\begin{aligned} & \inf_{\mathbb{Q}\in\Theta} \varepsilon(\mathbb{Q}, \mathbb{Q}_0) && (9)\\ \text{subject to} \quad & \mathbf{E}^{\mathbb{Q}}\left(e^{-rT_i} G_i(S_{T_i})\right) = C_i, \; i = 1, 2, \ldots, M. \end{aligned}$$

In order to connect to volatility, the relative entropy can be approximated by a pseudo-entropy function. Avellaneda et al. (1997) propose to approximate the entropy minimization problem (9) by a pseudo-entropy optimal control problem

$$\begin{aligned} & \min_\sigma \epsilon(\sigma, \sigma_0) \stackrel{\text{def}}{=} \mathbf{E}^{\mathbb{Q}}\left(\int_0^T \eta(\sigma^2(s))ds\right) \\ \text{subject to} \quad & \mathbf{E}^{\mathbb{Q}}\left(e^{-rT_i} G_i(S_{T_i})\right) = C_i, \; i = 1, 2, \ldots, M && (10)\\ & \sigma_{\text{lb}} \le \sigma_t \le \sigma_{\text{ub}} \end{aligned}$$

where $\sigma_{\text{lb}} > 0$, the pseudo-entropy function $\epsilon(\sigma, \sigma_0)$ is an approximation to the entropy $\varepsilon(\mathbb{Q}, \mathbb{Q}_0)$, $\mathbb{Q}$ is the measure defined by (2) with σ_t satisfying $\sigma_{\text{lb}} \le \sigma_t \le \sigma_{\text{ub}}$. The bound constraint $\sigma_{\text{lb}} \le \sigma_t \le \sigma_{\text{ub}}$ is necessary to guarantee that the class of diffusions is closed with respect to the topology of weak convergence of measures on continuous paths. See Avellaneda et al. (1997) for a more detailed discussion.

The choice of a PE function is not unique and its selection does not qualitatively affect calibration of a volatility function. Avellaneda et al. (1997) suggest a simple PE function below,

$$\eta(\sigma^2) \stackrel{\text{def}}{=} \frac{1}{2}(\sigma^2 - \sigma_0^2)^2, \tag{11}$$

where σ_0 is the prior volatility.

We propose to calibrate an uncertain volatility model (1) that it is consistent with given market bids and asks and is least committal to the missing information. Assume that there are two bounds $\sigma_{\min}$ and $\sigma_{\max}$ on volatility. For example, $\sigma_{\min}$ and $\sigma_{\max}$ can respectively be the historical lowest and highest volatilities or current lowest and highest implied volatilities. Since market makers would like to bid as low as possible, we determine the lower volatility bound $\underline{\sigma}$ in a volatility uncertainty model (1) as the minimum relative entropy distribution with the historical lowest volatility $\sigma_{\min}$ as a prior. In addition, to determine the lower volatility $\underline{\sigma}$ in an uncertain volatility model (1), it seems natural that the lower bound for the lower volatility $\underline{\sigma}$ is set to the historical low, i.e., $\underline{\sigma}_{\text{lb}} \equiv \sigma_{\min}$. Unfortunately, it is less clear how to set the upper bound $\underline{\sigma}_{\text{ub}}$ for the lower volatility $\underline{\sigma}$. We propose to set $\underline{\sigma}_{\text{ub}}$ to σ_{mid}, where σ_{mid} corresponds to a pricing measure which yields the bid and ask mid-prices. Subsequently we refer to σ_{mid} as the separating volatility.

Specifically, we propose to determine the lower volatility $\underline{\sigma}$ in an uncertain volatility model (1) by solving the optimization problem below,

$$\begin{aligned} & \min_{\underline{\sigma}} \mathbf{E}^{\mathbb{Q}}\left(\int_0^T \underline{\eta}(\underline{\sigma}_s^2)ds\right) \\ \text{subject to} \quad & \mathbf{E}^{\mathbb{Q}}(e^{-rT_i}G_i(S_{T_i})) = \underline{V}_i \\ & \underline{\sigma}_{\text{lb}} \leq \underline{\sigma}_t \leq \underline{\sigma}_{\text{ub}} \end{aligned} \tag{12}$$

where $\underline{\eta}$ is the pseudo entropy function below,

$$\underline{\eta}(\sigma^2) \stackrel{\text{def}}{=} \frac{1}{2}(\sigma^2 - \sigma_{\min}^2)^2, \quad \sigma_{\min} \stackrel{\text{def}}{=} \underline{\sigma}_{\text{lb}}, \quad \underline{\sigma}_{\text{ub}} \stackrel{\text{def}}{=} \sigma_{\text{mid}} \tag{13}$$

Note that the minimum relative entropy distribution being least committal to the missing information makes this estimation consistent with the idea behind an uncertain volatility model. In addition, the minimum volatility $\underline{\sigma}$ corresponds to a pricing measure which is consistent with today's market bid prices and is closest to the lowest volatility $\sigma_{\min}$.

An uncertain volatility model also requires that $\underline{\sigma} \leq \overline{\sigma}$. We achieve this by using the separating volatility σ_{mid} as the lower bound $\overline{\sigma}_{\text{lb}}$ for the upper volatility $\overline{\sigma}$ calibration: the upper volatility $\overline{\sigma}$ in an uncertain volatility model is determined from

$$\begin{aligned} & \min_{\overline{\sigma}} \mathbf{E}^{\mathbb{Q}}\left(\int_0^T \overline{\eta}(\overline{\sigma}_s^2)ds\right) \\ \text{subject to} \quad & \mathbf{E}^{\mathbb{Q}}(e^{-rT_i}G_i(S_{T_i})) = \overline{V}_i \\ & \sigma_{\text{mid}} \leq \overline{\sigma}_t \leq \sigma_{\max} \end{aligned} \tag{14}$$

where $\overline{\eta}$ is the pseudo entropy function:

$$\overline{\eta}(\sigma^2) \stackrel{\text{def}}{=} \frac{1}{2}(\sigma^2 - \sigma_{\max}^2)^2 \tag{15}$$

The maximum volatility $\overline{\sigma}$ then corresponds to a pricing measure which is consistent with today's market ask prices and is closest to the prior maximum volatility $\sigma_{\max}$.

In the entropy minimization problem (12), the prior volatility $\sigma_{\min}$ plays an important role in determining the lower volatility $\underline{\sigma}$ in an uncertain volatility model. Minimization of the specified pseudo-entropy function implies that the lower volatility $\underline{\sigma}$ deviates as little as possible from the volatility prior $\sigma_{\min}$ while ensuring consistency with the market bid price information. Similar remarks can be made about $\sigma_{\max}$ with respect to the upper volatility $\overline{\sigma}$.

3 A Lagrangian Approach

The pseudo-entropy minimization problems (10), (12), and (14) differ only in the specification of σ_0, $\sigma_{\rm lb}$, and $\sigma_{\rm ub}$. They are all optimal control problems with equality constraints which can be solved, as in Avellaneda et al. (1997), by maximizing the corresponding Lagragian functions.

To illustrate, we describe here the Lagrangian approach with respect to the pseudo-entropy minimization problem (10) for the lower volatility. Let Θ denote the set of all probability measures $\mathbb{Q}$ corresponding to the processes below

$$\frac{dS_t}{S_t} = (r-q)dt + \sigma_t dZ^{\mathbb{Q}}, \quad \text{where } 0 < \sigma_{\rm lb} \le \sigma_t \le \sigma_{\rm ub}$$

and $\epsilon(\sigma, \sigma_0)$ denotes the pseudo entropy approximation to $\varepsilon(\mathbb{Q}, \mathbb{Q}_0)$. The lower volatility bound $\underline{\sigma}$ is then determined by solving (10):

$$\begin{array}{ll} & \min_{\mathbb{Q}} \epsilon(\sigma, \sigma_0) \stackrel{\rm def}{=} \mathbf{E}^{\mathbb{Q}}\left(\int_0^T \eta(\sigma^2(s))ds\right) \\ \text{subject to} & \mathbf{E}^{\mathbb{Q}}\left(e^{-rT_i} G_i(S_{T_i})\right) = \underline{V}_i, \; i = 1, 2, \ldots, M \\ & \sigma_{\rm lb} \le \sigma_t \le \sigma_{\rm ub} \end{array}$$

Applying a Lagrangian approach for the equality constrained minimization problem, one considers

$$\inf_{\lambda} \sup_{\mathbb{Q}\in\Theta} \left(-\epsilon(\sigma, \sigma_0) + \sum_{i=1}^{M} \lambda_i \left(\mathbf{E}^{\mathbb{Q}}\left(e^{-rT_i} G_i(S_{T_i})\right) - \underline{V}_i \right) \right) \tag{16}$$

If the Lagrangian problem (16) has a solution, it is the optimal solution of (10). Following the stochastic control theory, Avellaneda et al. (1997) computes the optimum of the inner maximization problem by solving a nonlinear Hamilton-Jacobi-Bellman (HJB) equation.

The objective function of the Langrangian problem (16) can be unbounded from below if there is no feasible probability measure satisfying the equality constraints in (10). One computational difficulty with the Lagrangian approach (16) is that the Lagrangian function can be unbounded below due to infeasibility, possibility introduced by numerical error (or model error) in satisfaction of the equality constraints. Specification of $\sigma_{\rm lb}$ and $\sigma_{\rm ub}$ can affect this feasibility.

We illustrate this difficulty computationally with respect to the volatility calibration problem (10). Assume that the initial underlying price $S_0 = 100$, the risk free interest $r = 0.05$, and the dividend rate $q = 0.01$. We assume that the underlying price, under the risk neutral measure $\mathbb{Q}$, is governed by a constant elasticity of variance (CEV) model described in Cox & Ross (1976):

$$\frac{dS_t}{S_t} = (r-q)dt + \frac{\alpha}{S_t} dZ_t^{\mathbb{Q}} \tag{17}$$

where $\alpha = 15$, and $Z_t^{\mathbb{Q}}$ is a standard Brownian motion. Since the market is complete under a CEV model (17), option prices are uniquely determined. We assume that prices of 35 near-the-money options are computed from the assumed model and are available for calibration. See Table 2 in Appendix A for the strike price and option price description. The prior σ_0 is set to half of the minimum of the implied volatilities of selected options. The lower volatility bound σ_{lb} is set to the constant σ_0 and the upper volatility bound is the maximum of the exact local volatility function α/S and the constant σ_0, i.e.,

$$\sigma_{\text{ub}} = \max(\alpha/S, \sigma_0). \tag{18}$$

Here the upper bound σ_{ub} is floored by the constant σ_0 since the exact local volatility function goes to 0 as S approaches $+\infty$. However, all market prices correspond to near-the-money options and volatilities in the region far from S_0 are insignificant in pricing these options(see, e.g., Andersen & Brotherton-Ratcliffe (1998). This modification has little effect in pricing liquid options. Note that optimization problem (12) is mathematically feasible if the upper bound σ_{ub} equals the local volatility function $\frac{\alpha}{S}$ and the solution under the Lagrangian approach (16) exists. Computationally, on the other hand, the negligibly small numerical error destroyed the feasibility and led to the unboundedness of the Larangian problem. Our computational experience suggests that numerical error, which is responsible for infeasibility here, mainly arise from solving the nonlinear HJB PDE. The modification of the exact volatility function in (18) does not introduce significant numerical errors. Indeed we have also implemented the case when the exact local volatility is a constant and no modification of local volatility function is introduced in this case. The Lagrangian method also failed computationally to find the optimal solution to (10) in this case due to infeasibility caused by numerical error.

4 A Penalty Function Approach

To overcome numerical infeasibility in the Lagrangian (16) formulation, we consider instead a quadratic penalty function approach for the equality constraint in (10). This approach always yields a solution with the constraint approximately satisfied. Avellaneda, Buff, Friedman, Grandchamp, Kruk & Newman (2001) consider the quadratic penalty method for the entropy minimization problem when the state space Ω of underlying paths is discrete. We describe here the quadratic penalty approach in a continuous state space; the derivation and notations are similar to Avellaneda et al. (2001).

Instead of the Lagrangian formulation (16), we consider the following quadratic penalty formulation for (9):

$$\sup_{\mathbb{Q}\in\Theta} \left(-\varepsilon(\mathbb{Q}, \mathbb{Q}_0) - \frac{1}{2} \sum_{i=1}^{M} \frac{1}{w_i} \left(\mathbf{E}^{\mathbb{Q}} \left(e^{-rT_i} G_i(S_{T_i}) \right) - \underline{V}_i \right)^2 \right) \tag{19}$$

Here the dynamics of S_t is described by (2) and $\{w_i\}_{i=1}^M$ is a given vector of weights.

Problem (19) is a stochastic control problem. Unfortunately the stochastic control theory cannot be directly applied here since the second term in the objective function is not linear.

However, an equivalent problem, to which the stochastic control theory can be applied, can be derived. Denote

$$\chi_w^2 \stackrel{\text{def}}{=} \frac{1}{2}\sum_{i=1}^{M}\frac{1}{w_i}\left(\mathbf{E}^{\mathbb{Q}}\left(e^{-rT_i}G_i(S_{T_i})\right)-\underline{V}_i\right)^2. \tag{20}$$

From the Cauchy inequality, we have

$$\frac{1}{2}\lambda_i^2 w_i+\frac{1}{2w_i}\left(\mathbf{E}^{\mathbb{Q}}\left(e^{-rT_i}G_i(S_{T_i})\right)-\underline{V}_i\right)^2 \geq -\lambda_i\left(\mathbf{E}^{\mathbb{Q}}\left(e^{-rT_i}G_i(S_{T_i})\right)-\underline{V}_i\right) \quad \forall\lambda_i. \tag{21}$$

Thus

$$-\frac{1}{2}\sum_{i=1}^{M}\frac{1}{w_i}\left(\mathbf{E}^{\mathbb{Q}}\left(e^{-rT_i}G_i(S_{T_i})\right)-\underline{V}_i\right)^2 \leq \sum_{i=1}^{M}\lambda_i\left(\mathbf{E}^{\mathbb{Q}}\left(e^{-rT_i}G_i\right)-\underline{V}_i\right)+\frac{1}{2}\sum_{i=1}^{M}\lambda_i^2 w_i \quad \forall\lambda_i. \tag{22}$$

Using the above inequality, the objective function below is an upper bound for the objective function in (19),

$$\inf_{\lambda}\sup_{\mathbb{Q}\in\Theta}\left(-\varepsilon(\mathbb{Q},\mathbb{Q}_0)+\sum_{i=1}^{M}\lambda_i(\mathbf{E}^{\mathbb{Q}}\left(e^{-rT_i}G_i\right)-\underline{V}_i)+\frac{1}{2}\sum_{i=1}^{M}\lambda_i^2 w_i\right). \tag{23}$$

It can be shown that, under some reasonable assumptions, the above problem (23) is equivalent to problem (19), see Coleman, He & Li (2006) for more details.

Notice that the terms associated with the expectation $\mathbf{E}^{\mathbb{Q}}(\cdot)$ in problem (23) are now linear. Thus the stochastic control theory can be applied to derive a Hamilton-Jacobi-Bellman (HJB) equation. In contrast to the Lagrangian formulation (10), the objective function of (19) is convex and bounded from below. Thus the potential unboundedness problem in the Lagrangian formulation is avoided.

To solve the pseudo-entropy optimization problem corresponding to (23), an appropriate HJB equation can be applied based on stochastic control theory, similar to Proposition 2 in Avellaneda et al. (1997). Let

$$\Phi(X) = \sup_{\sigma_{\text{lb}}^2\leq\sigma^2\leq\sigma_{\text{ub}}^2}\left(\sigma^2 X-\eta(\sigma^2)\right). \tag{24}$$

Given a vector of real numbers $\lambda=(\lambda_1,\lambda_2,\ldots,\lambda_M)$, let $W(S,t,\lambda)$ be the solution to

$$\begin{aligned} W_t \quad &+ \quad e^{rt}\Phi\Big(\frac{e^{-rt}}{2}S^2W_{SS}\Big)+(r-q)SW_S-rW = \\ &- \sum_{t<T_i\leq T}\lambda_i\delta(t-T_i)\left(G_i(S)-e^{rT_i}\underline{V}_i+\frac{1}{2}e^{rT_i}\lambda_i w_i\right), \quad S>0, \quad t\leq T \end{aligned} \tag{25}$$

with the final condition $W(S, T+0, \lambda) = 0$ where $\delta(\cdot)$ is a Dirac function. Then it can be shown that

$$
\begin{aligned}
& W(S,t,\lambda) \qquad\qquad\qquad\qquad\qquad\qquad\qquad\qquad\qquad\qquad\qquad\qquad\qquad\qquad\qquad\qquad (26) \\
= \; & \sup_{\mathbb{Q}\in\Theta} \left\{ \mathbf{E}_t^{\mathbb{Q}} \left[-e^{rt} \int_t^T \eta(\sigma_s^2) ds \right] + \sum_{t<T_i\le T} \mathbf{E}_t^{\mathbb{Q}} \left[\lambda_i \left(e^{-r(T_i-t)} G_i - e^{rt} \underline{V}_i + \frac{1}{2} e^{rt} \lambda_i w_i \right) \right] \right\}.
\end{aligned}
$$

Moreover, the supremum in (26) is realized by the diffusion process

$$\frac{dS_t}{S_t} = (r-q)dt + \sigma^*(S,t) dZ_t^{\mathbb{Q}^*} \tag{27}$$

where $\sigma^*(S,t)$ is the following function of S and t:

$$(\sigma^*(S,t))^2 = \Phi'(\frac{e^{-rt}}{2} S^2 W_{SS}). \tag{28}$$

This analysis shows that the optimal control problem (23) can be solved via

$$\inf_{\lambda\in\Re^M} W(S_0, 0, \lambda). \tag{29}$$

where $W(S_0, 0, \lambda)$ is computed by solving the HJB nonlinear partial differential equation (25).

Since the objective function in the optimization problem (26) is a convex function of λ, the optimization problem (29) is convex. We apply a BFGS method for minimization problem (29), see, e.g., Fletcher (1987) for detailed discussion on BFGS. Note that the BFGS method requires computation of function as well as the first order derivatives; however computation of a Hessian matrix is not required.

Let $W_i(S,t,\lambda)$ denote the derivative of W with respect to λ_i, i.e.,

$$W_i(S,t,\lambda) = \frac{\partial W}{\partial \lambda_i}.$$

Then $W_i(S,t,\lambda)$ can be determined by taking derivative with respect to λ_i in equation (25), i.e.,

$$
\begin{aligned}
(W_i)_t + \frac{1}{2}\Phi'\left(\frac{e^{-rt}}{2} S^2 W_{ss}\right) S^2 (W_i)_{ss} + (r-q) S (W_i)_s - rW_i = \\
-\delta(t-T_i)\left(G_i(S) - e^{rT_i}\underline{V}_i + e^{rT_i}\lambda_i w_i\right).
\end{aligned} \tag{30}
$$

According to the definition (11) of $\eta(\cdot)$, $\Phi(\cdot)$ and $\Phi'(\cdot)$ are given below,

$$
\Phi(X) = \begin{cases}
\frac{1}{2}X^2 + \sigma_0^2 X, & \text{if } \sigma_{\text{lb}}^2 - \sigma_0^2 < X < \sigma_{\text{ub}}^2 - \sigma_0^2, \\
\sigma_{\text{lb}}^2 X - \frac{1}{2}(\sigma_{\text{lb}}^2 - \sigma_0^2)^2, & \text{if } X \le \sigma_{\text{lb}}^2 - \sigma_0^2, \\
\sigma_{\text{ub}}^2 X - \frac{1}{2}(\sigma_{\text{ub}}^2 - \sigma_0^2)^2, & \text{if } X \ge \sigma_{\text{ub}}^2 - \sigma_0^2,
\end{cases} \tag{31}
$$

and

$$\Phi'(X) = \begin{cases} X + \sigma_0^2, & \text{if } \sigma_{\text{lb}}^2 - \sigma_0^2 < X < \sigma_{\text{ub}}^2 - \sigma_0^2, \\ \sigma_{\text{lb}}^2, & \text{if } X \le \sigma_{\text{lb}}^2 - \sigma_0^2, \\ \sigma_{\text{ub}}^2, & \text{if } X \ge \sigma_{\text{ub}}^2 - \sigma_0^2. \end{cases} \tag{32}$$

Assume now that $W(S, 0, \lambda)$ obtains a minimum at $\lambda^* = \{\lambda_i^*\}_{i=1}^M$. From equation (28), (30), and the first order optimality condition,

$$\mathbf{E}^{\mathbb{Q}^*}\left(e^{-rT_i} G_i(S_{T_i}) - \underline{V}_i\right) = -\lambda_i^* w_i. \tag{33}$$

Here $\{w_i\}_{i=1}^M$ is the given weight vector and the expectation $\mathbf{E}^{\mathbb{Q}^*}$ is with respect to S_t which solves the stochastic differential equation (27). Equation (33) relates each calibration error in the option V_i to the corresponding weight w_i and multiplier λ_i^*.

Next we discuss how to solve the nonlinear HJB partial differential equation (25) computationally. Once a solution $W(S, t, \lambda)$ to (25) is computed, $\Phi(\cdot)'$ can be determined and the derivatives W_i can be computed from the linear PDE (30). Avellaneda et al., (1997, 1995), use a trinomial method, which is an explicit scheme for solving a HJB partial differential equation. Unfortunately, a trinomial method may not converge to the correct solution of equation (25) in practice. Moreover, the solution from a trinomial method does not naturally provide information for the volatility function outside a triangular region of discretization grid points in (S, t).

Pooley, Forsyth & Vetzal (2003) propose a monotone method for solving the *Black-Scholes-Barenblatt* (BSB) nonlinear PDE. Unfortunately their convergence analysis does not directly apply to the more complex HJB equation (25). Comparing HJB equation (25) to a BSB equation, we see that the coefficient of W_{SS} becomes more complicated. In our implementation, we use the Newton method directly for the finite difference equation for (25). The Newton method is locally quadratically convergent in solving the algebraic equation at each time step. Since a HJB equation (25) is nonlinear, one needs to investigate whether the numerical solution converges to the correct solution of the nonlinear PDE. It can be shown that, using the fully implicit method, the exact solutions to the finite difference equations converge to the viscosity solution of equation (25). We refer an interested reader to the analysis in Coleman et al. (2006).

To illustrate the main advantage of using the penalty function approach for the entropy minimization problem (9), we now consider the same calibration example discussed in §3. In contrast to the Lagrangian method, which fails to provide a solution for this example, the quadratic penalty function approach is able to produce an approximation which satisfies the equality constraint approximately. Figure 1 displays the volatility function calibrated from option prices described in Table 2 in Appendix B, using the quadratic penalty method with a weight vector of all ones. The largest calibration error is 0.0119 and the mean of the error is 0.0018. The calibrated volatility function and the exact volatility function across underlying prices at different times are graphed in Figure 2. These graphs suggest that the calibrated volatility function accurately approximate the true volatility when S is close to S_0 except for several troughs when t is near some maturity time T_i.

Similar to Avellaneda et al. (1997), the appearance of troughs in Figure 1 & 2, when t is near a maturity of a given option, can be explained based on the following interesting observations on the solution to optimality in problem (29) and PDE(25).

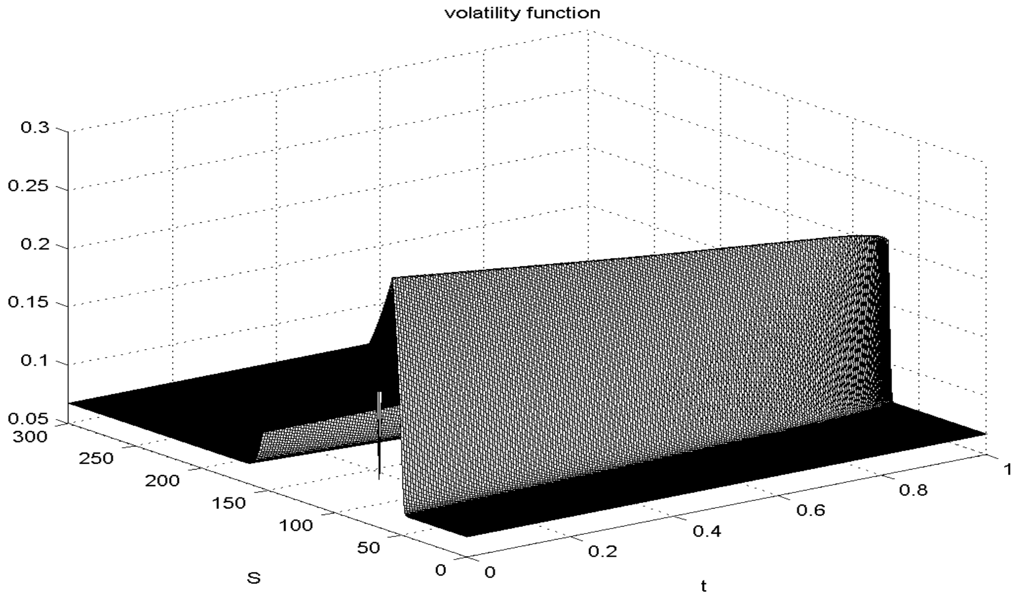

Figure 1: A local volatility function calibrated by the penalty method

Denote

$$\tilde{W} = e^{-rt}W \quad \text{and} \quad \tilde{S} = e^{-(r-q)t}S.$$

The PDE (25) becomes

$$\tilde{W}_t + \Phi\left(\frac{1}{2}\tilde{S}^2\tilde{W}_{\tilde{S}\tilde{S}}\right) = -\sum_{t<T_i\le T}\lambda_i\delta(t-T_i)\left(e^{-rT_i}G_i(e^{(r-q)T_i}\tilde{S}) - \underline{V}_i + \frac{1}{2}\lambda_i w_i\right) \tag{34}$$

Consider the standard option payoff function $G_i(S)$. Differentiating equation (34) with respect to $\tilde{S}$ twice,

$$\tilde{\Gamma}_t + \left[\Phi(\frac{1}{2}\tilde{S}^2\tilde{\Gamma})\right]_{\tilde{S}\tilde{S}} = -\sum_{t<T_i\le T}\lambda_i\delta(t-T_i)e^{-qT_i}\delta(\tilde{S} - e^{-(r-q)T_i}K_i) \tag{35}$$

where $\tilde{\Gamma} = \tilde{W}_{\tilde{S}\tilde{S}} = e^{(r-2q)t}W_{SS}$. From (28), we have

$$(\sigma^*(S,t))^2 = \Phi'\left(\frac{1}{2}\tilde{S}^2\tilde{\Gamma}\right). \tag{36}$$

Let λ^* be the minimizer of the optimization problem (29), let $W^*(S,t) = W(S,t,\lambda^*)$ be the optimal objective function in the space (S,t), and let $\sigma^*(S,t)$ be the associated volatility function. From (36), $\sigma^*(S,t)$ is determined by $\tilde{\Gamma}^*$. As discussed in Avellaneda et al. (1997), $\tilde{\Gamma}^*$ is singular at point $(S,t) = (S_i,T_i)$ and quickly diffuses into a smooth function away from (S_i,T_i).

If $\lambda_i^* = 0$ for all i, the right hand of the equation (35) is zero. From the final condition $\tilde{\Gamma}(\tilde{S},T+) = 0$, $\tilde{\Gamma}^* \equiv 0$ is a solution to (35). In fact, it can be shown that $\tilde{\Gamma}^* \equiv 0$ is the unique solution to (36); see Coleman et al. (2006). By definition (31) of $\Phi(\cdot)$, we have $\sigma^*(S,t) \equiv \sigma_0$

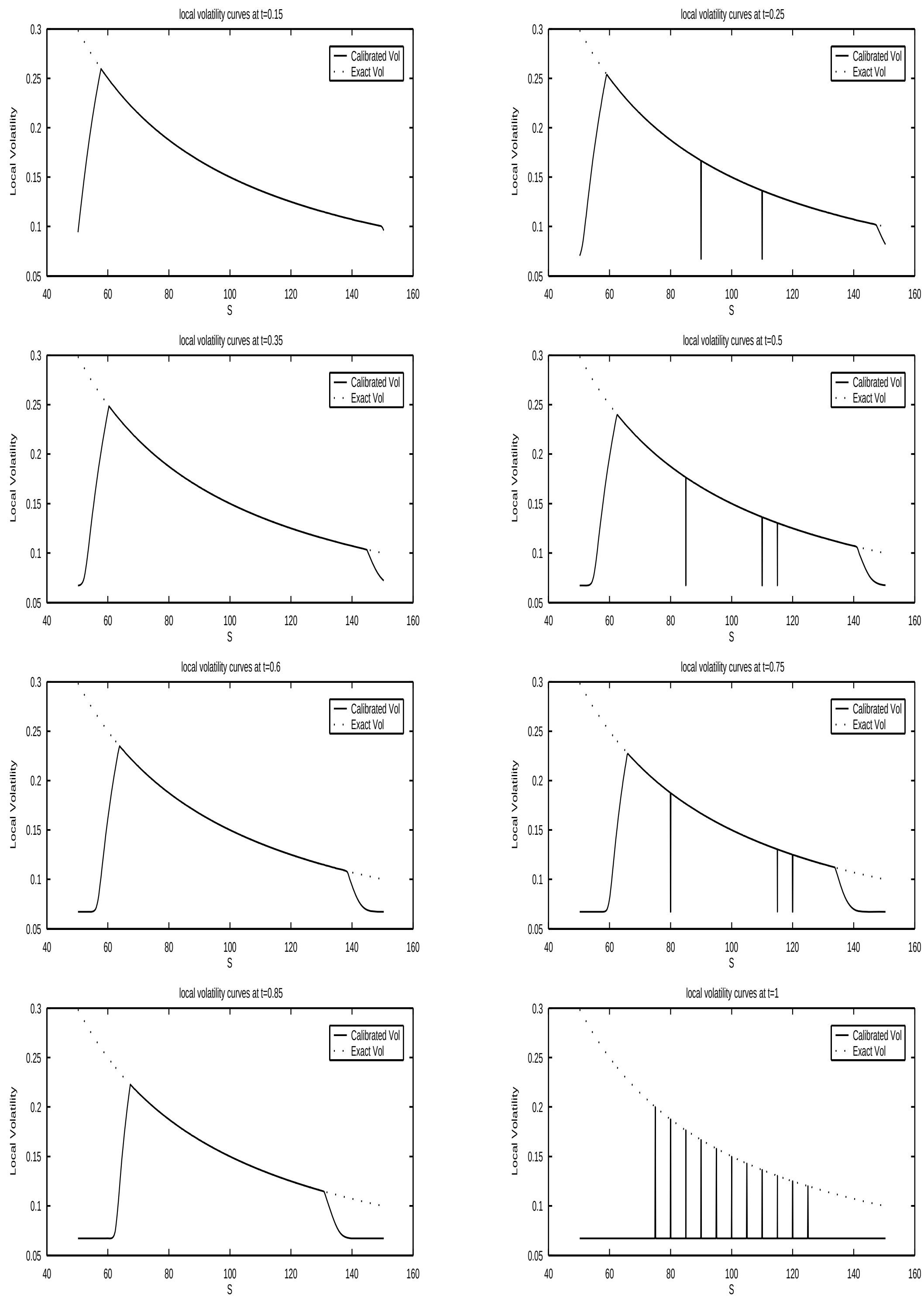

Figure 2: The calibrated volatility function and the exact volatility function at different times based on the entropy minimization (16) with $w_i \equiv 1$, $\sigma_0 = \sigma_{\text{lb}} = 0.5 \min(\{\sigma_{\text{impv}}\})$ and $\sigma_{\text{ub}} = \max(\alpha/S, 0.5 \min(\{\sigma_{\text{impv}}\}))$ where σ_{impv} are implied volatilities. Pictures on the right are volatility curves at maturity times T_i. Pictures on the left are volatility curves when time t is between maturity times.

and the pseudo-entropy $\epsilon(\sigma^*, \sigma_0) = 0$. From (33), we conclude that the calibration error of each option is identically zero. This means that the prior volatility σ_0 can perfectly price all given options. However, a constant prior σ_0 in practice cannot be expected to price all given options exactly. Therefore let us consider now the case when $\{\lambda_i^*\}$ are not identically zero. Each nonzero λ_i^* is associated with a Dirac source in (35). Assume that each payoff function $G_i(S)$ is convex, e.g., a standard European option. If $\lambda_i^* > 0$, a positive Dirac source on $\tilde{\Gamma}^*$ is expected at $(S,t) = (K_i, T_i)$. From the definition (32) of $\Phi'(\cdot)$, $\sigma^*(K_i,T_i) = \sigma_{\rm ub}(K_i,T_i)$. Similarly, if $\lambda_i^* < 0$, $\tilde{\Gamma}^*$ has a negative Dirac source at $(S,t) = (K_i,T_i)$ and $\sigma^*(K_i,T_i) = \sigma_{\rm lb}(K_i,T_i)$. The troughs observed in Figure 2 correspond to negative λ_i^* and thus over-pricing of the ith option from (33). Similarly ridges correspond to positive λ_i^* and thus under-pricing of the ith option.

5 Calibrating and Pricing Under an UVM

We now illustrate characteristics of the minimum and maximum volatility functions $\underline{\sigma}$ and $\overline{\sigma}$ for an uncertain volatility model (1), calibrated from bid and ask pairs. In addition, using the calibrated uncertain volatility model, we price bid-ask spreads of standard options with different strikes and maturities as well as some exotic options. We compare the bid and ask spreads generated by the calibrated uncertain volatility model with the spreads produced by an uncertain volatility model with a constant volatility interval, specified using the minimum and maximum implied volatilities. We observe that the calibrated uncertain volatility model, which is consistent with the market, generates more reasonable price intervals. In §5.1 we first consider a synthetic market where the bid and ask prices are generated based on a constant elasticity of variance (CEV) model as in §3. The calibrated uncertain volatility model from S&P 500 market prices is illustrated in §5.2.

5.1 Calibration from Prices of a CEV Model

To illustrate, we first assume that bid and ask prices for European options are generated according to the CEV model (17) considered in §3. We assume here that the spread level is a monotone function of maturity as listed in Table 1 and bid and ask prices are specified as follows,

$$\underline{V} = V - \tfrac{1}{2}\text{spread}, \quad \text{and} \quad \overline{V} = V + \tfrac{1}{2}\text{spread} \tag{37}$$

where the mid-price V are computed according to the assumed CEV model (17). Let $\sigma_{\rm bid}$ and $\sigma_{\rm ask}$ denote the implied volatilities corresponding to the bid and ask prices respectively.

To calibrate an uncertain volatility model, the priors $\sigma_{\min}$ and $\sigma_{\max}$ are chosen to represent the lowest and highest volatilities. To illustrate, here we simply set priors as percentages of the implied volatilities: the prior $\sigma_{\min} = 0.2\min(\{\sigma_{\rm bid}\})$ and the prior $\sigma_{\max} = 2\max(\{\sigma_{\rm ask}\})$. In practice perhaps a more reasonable choice is historic extreme volatilities. The separating volatility $\sigma_{\rm mid}$ is calibrated from the mid-prices using a spline representation as in Coleman et al. (1999). From the penalty function formulation (19), the calibration errors are expected to decrease as weights decrease. For computational examples in this paper, the calibration error is relatively small when weights are all ones, with the maximum calibration error equal

Table 1: Bid and Ask Spreads

Maturity(T)	Spread($)
0.1	0.10
0.25	0.12
0.5	0.14
0.75	0.18
1	0.20

to 0.005. We refer an interested reader to Coleman et al. (2006) for more discussion on sensitivity of calibration errors to weights.

The volatility surfaces $\underline{\sigma}$ and $\overline{\sigma}$, for an uncertain volatility model calibrated from bid-ask prices described (with uniformly weights of ones), are graphed in Figure 3. The calibrated volatility functions are close to the assumed local volatility function in the CEV model in a significant region centered on the hyperplane $S = S_0$. As S moves sufficiently away from $S = S_0$, the volatility surfaces gradually approach the corresponding priors and eventually become flat and equal to the priors. This is reasonable since near the money options contain little information on volatility as S moves away from S_0.

Figure 4 plots volatility intervals across underlying prices at different times. We observe more separation between volatility function bounds $\underline{\sigma}$ and $\overline{\sigma}$ near $t = 0$. This is partly because fewer liquid option prices with shorter maturities are assumed to be given, as is typically the case of available market data. In addition, bid and ask prices contain little information on volatility far away from the initial underlying prices. Similar to the example in §4, we observe *troughs* in the minimum volatility function $\underline{\sigma}$. We also observe *ridges* in the maximum volatility function $\overline{\sigma}$. As in §4, troughs in the minimum volatility function correspond to model prices slightly higher than the bid prices. Ridges in the maximum volatility function, on the other hand, correspond to model prices slightly lower than the ask prices.

While mid-prices are used to calibrate a single volatility surface in a local volatility function model, bid and ask pairs are used directly here for uncertain volatility model calibration. In addition, two model calibration problems differ in the specification of priors. In the local volatility function calibration problem, the prior represents the most likely value for volatility. In the proposed calibration of an uncertain volatility model here, the prior for the lower volatility correspond to the lowest volatility value; thus this prior can be set, e.g., to the lowest historic volatility. The minimum volatility function $\underline{\sigma}$ in Figure 4 deviates further from the given CEV volatility function in a relatively large region when time is close to 0. The local volatility function calibrated from the middle price, on the other hand, fits the given volatility function in larger regions, see Figure 2.

Next we compare the price intervals from an uncertain volatility model, calibrated from bid and ask pairs, with price intervals from an uncertain volatility model for which the constant volatility bounds are specified by the minimum and maximum implied volatilities of the given mid-prices, respectively. We first compare spreads of European call options for different strikes and maturities.

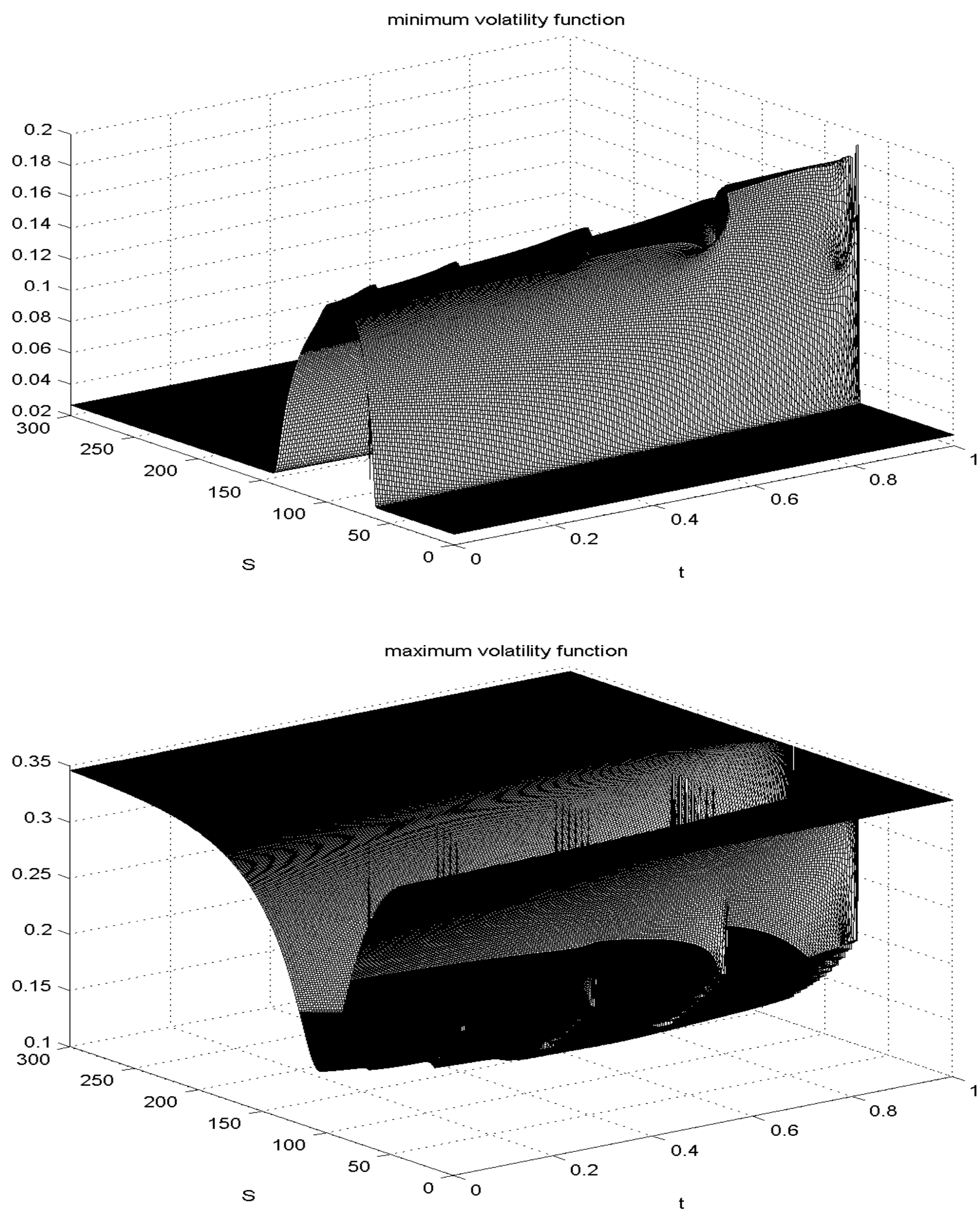

Figure 3: Minimum and maximum local volatilities calibrated from the CEV example. The separating volatility σ_{mid} is determined using a spline with knots at $[80, 90, 100, 110, 120] \times [0.25, 0.75]$.

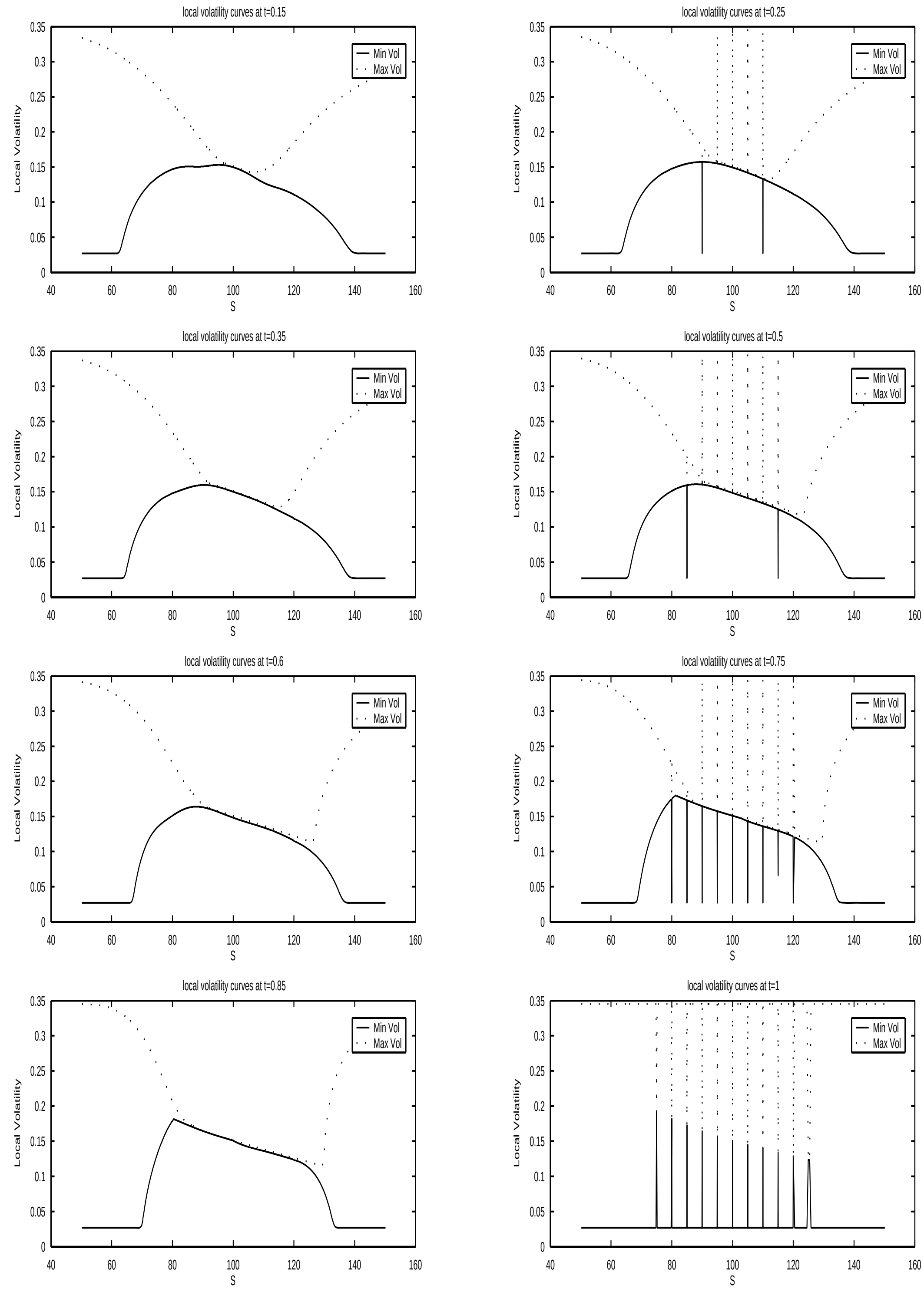

Figure 4: Minimum and maximum local volatilities from the CEV example: σ_{mid} is computed from the mid-prices using a spline function. Pictures on the right are lower and upper volatility curves at maturity times T_i. Pictures on the left are volatility curves between maturity times.

Figure 5 graphs the implied volatilities, corresponding to bid and ask prices, respectively, generated from the calibrated uncertain volatility model for which the volatility bounds are graphed in Figure 3. For comparison, we also graphed the implied volatilities corresponding to the bid and ask prices from an uncertain volatility model with constant volatility bounds. Specifically, the circle-curve and the asterisk-curve represent implied volatilities of bid and ask prices computed under the calibrated uncertain volatility model. The solid and the dash lines represent the implied volatilities of bid and ask prices, which correspond to the UVM model with a constant volatility interval from the extreme implied volatilities. Specifically the benchmark uncertain volatility model with a constant bounds has $\underline{\sigma} = \min\{(\sigma_{\text{impv}})_{\text{bid}}\}$ and $\overline{\sigma} = \max\{(\sigma_{\text{impv}})_{\text{ask}}\}$.

From Figure 5, we observe that the spreads computed under the calibrated uncertain volatility model are much smaller than those priced under the uncertain volatility model with the constant volatility bounds, especially in the near-the-money region, For deeply out-the-money options and deeply in-the-money options, the spreads computed under the calibrated uncertain volatility model become larger because $\underline{\sigma}$ and $\overline{\sigma}$ approach to two priors, which form a larger volatility interval than the price pairs from the simple UVM using two extreme implied volatilities. This is intuitively reasonable, since the volatility gradually becomes more uncertain as the underlying price moves further away from the current price.

In addition to pricing illiquid standard options, a calibrated uncertain volatility model can be used to price and hedge exotic options. Next we compare, the price spreads of barrier options from the calibrated uncertain volatility model with those produced by an uncertain volatility model with the constant volatility bounds from extreme implied volatilities. Specifically we use the calibrated uncertain volatility model to produce the price spreads of an up-and-out barrier call option with the strike $K = 100$ and the barrier $H = 120$. (Interest rate and dividend rate are assumed to be the same as before.) Figure 6 compares the spreads generated from the calibrated uncertain volatility model, as a function of the underlying value, with the spreads from the uncertain volatility model with a constant volatility interval from extreme implied volatilities. Under the calibrated uncertain volatility model, the maximum spread is about 0.385. For the uncertain volatility model with a constant volatility interval, where $\underline{\sigma} = \min\{(\sigma_{\text{impv}})_{\text{bid}}\}$ and $\overline{\sigma} = \max\{(\sigma_{\text{impv}})_{\text{ask}}\}$, the spread can be larger than \$3.5. This example illustrates that the calibrated uncertain volatility model yields more realistic price spreads for illiquid standard options as well as exotic options.

5.2 Calibration from S&P500 Index Option Bid and Ask Prices

In this section we illustrate calibration of an uncertain volatility model from S&P500 index option market bid and ask prices on April 20, 1999. We use the same price data described in Andersen & Andreasen (2000); implied volatilities corresponding to bid and ask prices are given in Table 3 in Appendix A. The initial index is $S_0 = 1306.17$, the risk free interest rate is 0.0559, and the dividend rate is 0.0114.

When calibrating an uncertain volatility model from the given data, we set the priors for the minimum local volatility $\underline{\sigma}$ and the maximum local volatility $\overline{\sigma}$ to percentages of the minimum and maximum implied volatilities of bid and ask prices respectively. Specifically, $\sigma_{\min} = 0.5 \min\{\sigma_{\text{bid}}\}$ in the entropy minimization problem (12) for the minimum local volatility $\underline{\sigma}$. Similarly, the prior $\sigma_{\max} = 1.5 \max\{\sigma_{\text{ask}}\}$ in the entropy minimization problem for the

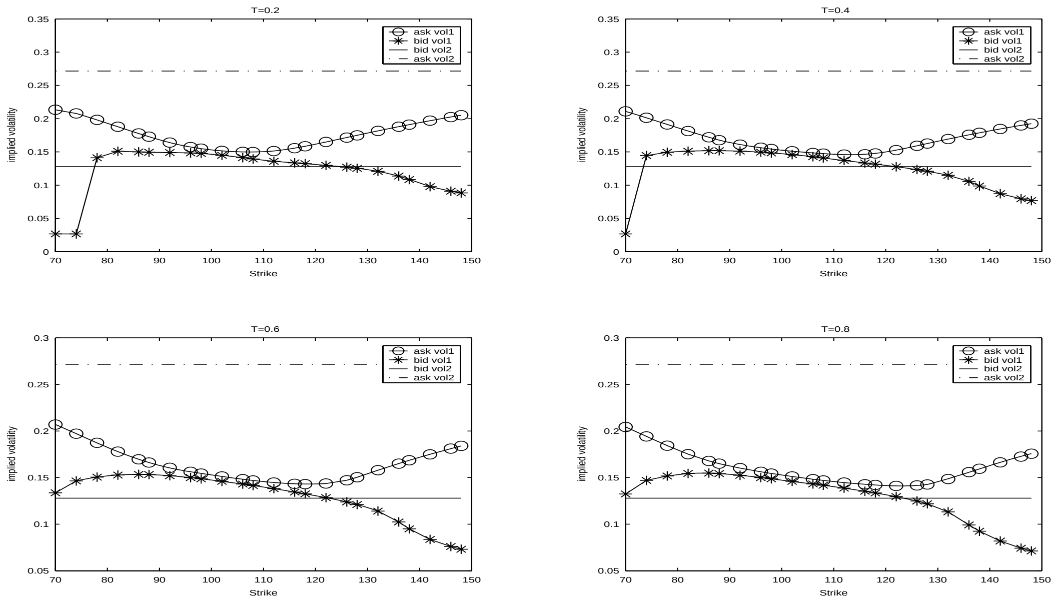

Figure 5: Comparing spreads of standard European options from the calibrated uncertain volatility model with the uncertain volatility model with simple constant volatility bounds. The curves "ask vol1" and "bid vol1" are implied volatilities from the extreme prices computed with the uncertain volatility model calibrated to the given bid and ask prices. The curve "ask vol2" corresponds to the maximum of implied volatilities of ask prices and "bid vol2" corresponds to the minimum of the implied volatilities of bid prices.

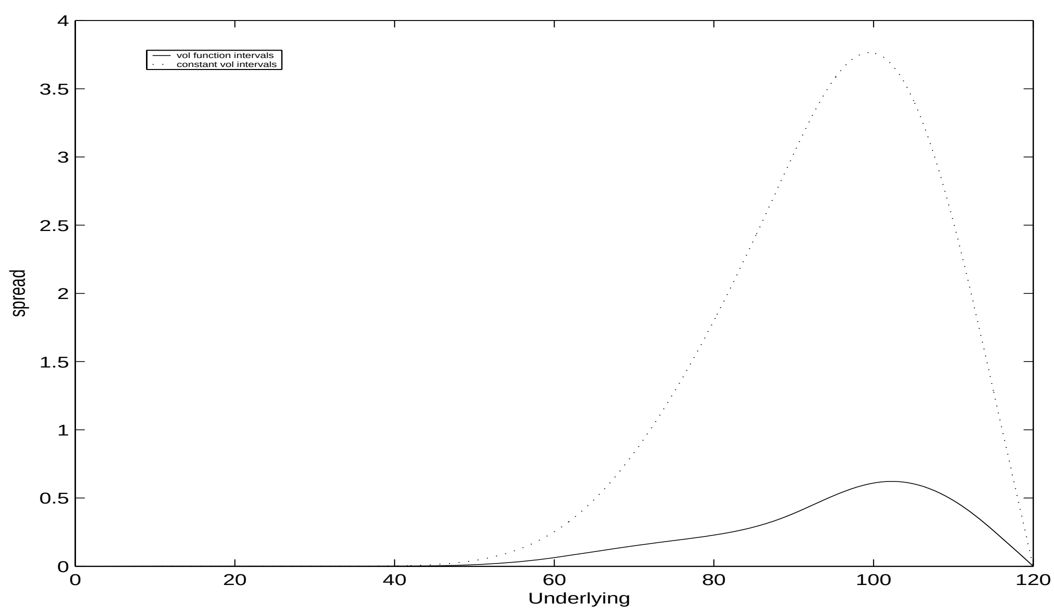

Figure 6: Price spreads of an up-and-out barrier option with $K = 100$ and $H = 110$ for the UVM with $[\underline{\sigma}, \overline{\sigma}] = [\min\{\sigma_{\rm bid}\}, \max\{\sigma_{\rm ask}\}]$ and the uncertain volatility model with the calibrated volatility functions shown in Figure 4.

upper bound local volatility $\overline{\sigma}$. The separating volatility σ_{mid}, which is used to ensure $\underline{\sigma} \leq \overline{\sigma}$, is estimated from the implied volatilities of option mid-prices as before. We implement this estimation using a spline representation for σ_{mid} with the knots placed on a rectangular mesh $[0 : 0.25 : 1] \times [0.8S_0 : 0.06S_0 : 1.4S_0]$. The maximum calibration error to the mid-prices is 0.014.

Figure 7 illustrates the minimum volatility $\underline{\sigma}$ and the maximum volatility $\overline{\sigma}$ for the uncertain volatility model calibrated from the given market bid and ask prices on April 20, 1999. As in §5.1, we use the weight vector of all ones. The maximum calibration errors to the bid prices and ask prices are 0.0624 and 0.0244 respectively. The volatility intervals are plotted in Figure 8. Similar to the CEV model example, troughs and ridges can be observed for $\underline{\sigma}$ and $\overline{\sigma}$ respectively. In addition, the lower volatility $\underline{\sigma}$ and $\overline{\sigma}$ become more and more separated as time approaches zero.

Figure 9 compares bid-ask prices for an up-and-out barrier option with strike $K = 1306.17$ and barrier $H = 1.1K$ from the uncertain volatility model calibrated from bid-ask prices with those from the uncertain volatility model with a constant volatility interval $[\underline{\sigma}, \overline{\sigma}] = [\min\{\sigma_{\text{bid}}\}, \max\{\sigma_{\text{ask}}\}]$. In contrast to the prices from the calibrated uncertain volatility model from the bid-ask prices, the price pairs for the uncertain volatility model with the constant interval $[\underline{\sigma}, \overline{\sigma}] = [\min\{\sigma_{\text{bid}}\}, \max\{\sigma_{\text{ask}}\}]$ seem to be unrealistically large. In addition, the uncertain volatility model calibrated from bid and ask prices is obtained to be consistent with the market bid and ask prices of liquid options whereas an uncertain volatility model with a constant volatility interval ensures no consistency with the market bid and ask price information.

6 Conclusion

The volatility smile has been well documented; this suggests that the classical Black-Scholes is inadequate in option modeling. In addition, difficulty in volatility estimation and empirical evidence suggests the presence of volatility risk. An uncertain volatility model proposed by Avellaneda et al. (1995) is an alternative option pricing model, yielding a pair of extreme prices for a derivative contract which naturally correspond to bid and ask prices.

To successfully price and manage option risk under an uncertain volatility model, it is important that the model is consistent with liquid bid and ask prices available in the market. An uncertain volatility model with a simple constant volatility bounds from extreme volatilities tends to yield price pairs inconsistent with market observations and can generate unrealistically large price intervals.

Calibrating an uncertain volatility model from the liquid market bid and ask prices is a challenging problem both mathematically and computationally. The market option information is generally insufficient to determine a sufficiently complex uncertain volatility model which is consistent with market information.

Consistent with volatility uncertainty, which is the principal idea behind an uncertain volatility model, we propose an entropy minimization approach. This approach allows estimation of an uncertain volatility model with volatility bounds least biased with respect to missing information. We discuss mathematical and computational challenges in calibrating the volatility bounds in an uncertain volatility model from bid and ask prices. In particular,

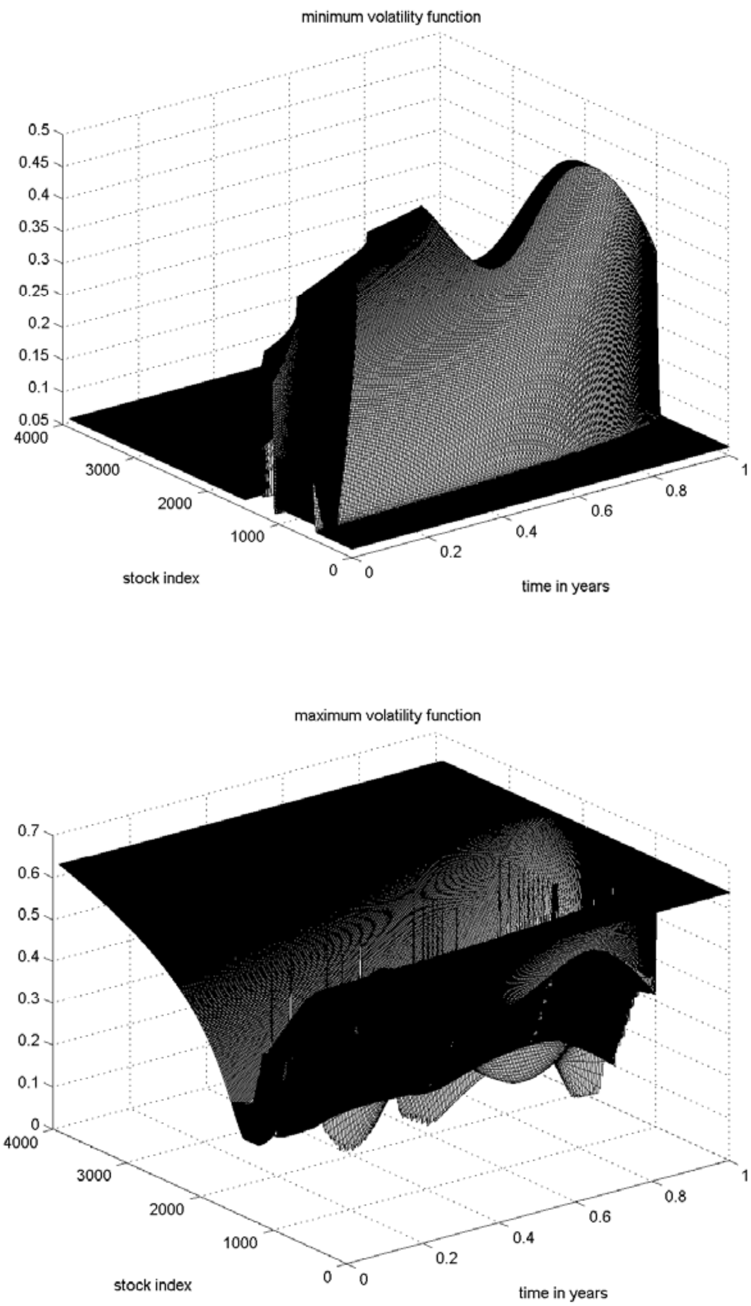

Figure 7: Volatility function bounds $\underline{\sigma}$ and $\overline{\sigma}$ calibrated from S&P 500 market data on April 20, 1999.

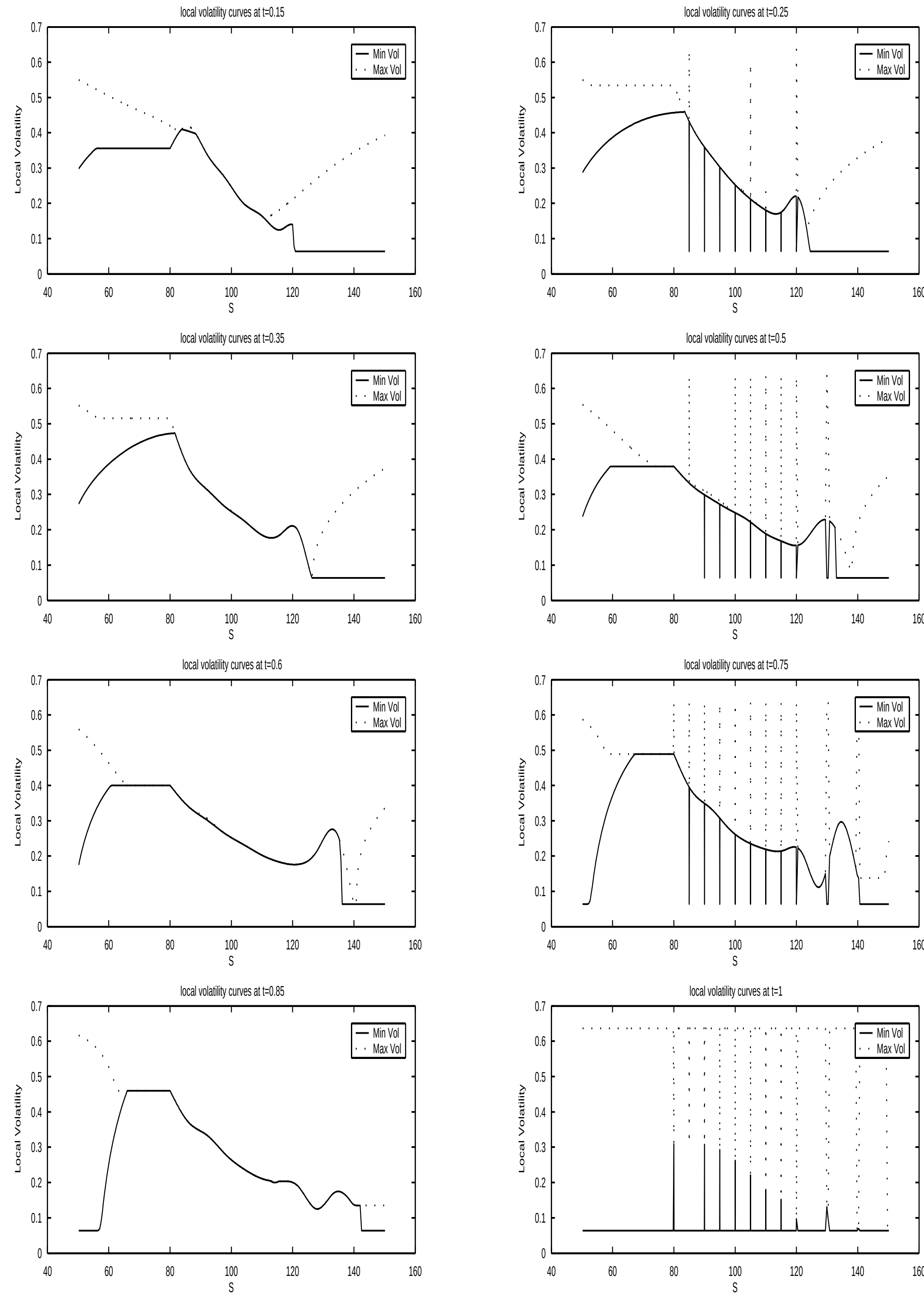

Figure 8: Volatility bounds $\underline{\sigma}$ and $\overline{\sigma}$, at different times, calibrated from the S&P 500 market data on April 20, 1999. Pictures on the right are volatility curves at a maturity time T_i. Pictures on the left are volatility curves at time between maturities.

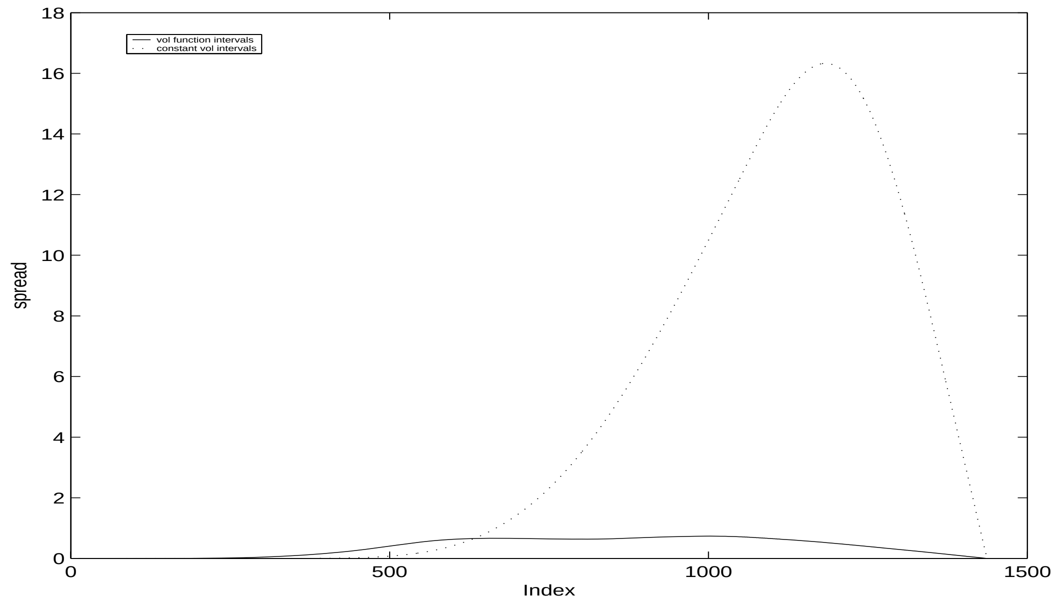

Figure 9: Price spreads of an up-and-out barrier option with $S_0 = 1306.7$, $K = 1306.17$ and $H = 1.1K$ from the uncertain volatility model with $[\underline{\sigma}, \overline{\sigma}] = [\min\{\sigma_{\text{bid}}\}, \max\{\sigma_{\text{ask}}\}]$ and price spreads from the calibrated uncertain volatility model with $\underline{\sigma}$ and $\overline{\sigma}$ shown in Figure 7.

a quadratic penalty approach is considered in this paper to avoid potential unboundedness (due to computational infeasibility) in entropy minimization problems.

We illustrate the calibrated uncertain volatility model from the proposed method using both a set of synthetic bid and ask prices generated from a CEV model as well as a set of the S&P 500 index option data on April 20, 1999. In both cases, we observe that the difference between the calibrated volatility bounds increases as the underlying price deviates from the current price. This seems to be naturally consistent with the fact that only near-the-money option price information is available. In addition, for a given underlying price, the difference between volatility bounds tend to increase as time decreases. This is also reasonable since initially the underlying price S is unlikely to deviate far from the current value S_0; thus option values contain less information on volatility initially when underlying value is far from S_0.

In addition, we compare the bid and ask price pairs, yielded from the calibrated uncertain volatility model with bid and ask prices from an uncertain volatility model with constant volatility bounds, e.g., from extreme implied volatilities. We illustrate that, while the latter often yields unrealistic price pairs, the price pairs from the calibrated model are more realistic and are consistent with given market information.

References

Andersen, L. & Andreasen, J. (2000), 'Jump-diffusion processes: Volatility smile fitting and numerical methods for option pricing', *Review of Derivative Research* **4**, 231–262.

Andersen, L. & Brotherton-Ratcliffe, R. (1998), 'The equity option volatility smile: an implicit finite difference approach', *Journal of Computational Finance* **1**(2), 5–32.

Avellaneda, M., Buff, R., Friedman, C., Grandchamp, N., Kruk, L. & Newman, J. (2001), 'Weighted monte carlo: A new technique for calibrating asset-pricing models', *International Journal of Theoretical and Applied Finance* **4**(1), 91–119.

Avellaneda, M., Friedman, C., Holemes, R. & Samperi, D. (1997), 'Calibrating volatility surfaces via relative entropy minimization', *Applied Mathematical Finance* **4**, 37–64.

Avellaneda, M., Levy, A. & Paras, A. (1995), 'Pricing and hedging derivative securities in markets with uncertain volatilities', *Applied Mathematical Finance* **2**, 73–88.

Avellaneda, M. & Paras, A. (1996), 'Managing the volatility risk of portfolios of derivative securities: the Lagrangian uncertain volatility model', *Applied Mathematical Finance* **3**, 21–52.

Bakshi, G., Cao, C. & Chen, Z. (1997), 'Empirical performance of alternative option pricing models', *Journal of Finance* **52**, 2003–2049.

Buchen, P. W. & Kelly, M. (1996), 'The maximum entropy distribution of an asset inferred from option prices', *The Journal of Financial and Quantitative Analysis* **31**(1), 143–159.

Coleman, T. F., He, C. & Li, Y. (2006), 'Computation and analysis for a constrained entropy optimization problem in finance', *Submitted to Journal of Computational and Applied Mathematics: A Special Issue on Numerical PDE Methods in Finance* .

Coleman, T. F., Kim, Y., Li, Y. & Verma, A. (2001), 'Dynamic hedging with a deterministic volatility function model', *The Journal of Risk* **4**(1), 63–90.

Coleman, T. F., Li, Y. & Verma, A. (1999), 'Reconstructing the unknown local volatility function', *The Journal of Computational Finance* **2**(3), 77–102.

Cover, T. M. & Thomas, J. A. (1991), *Elements of Information Theory*, John Wiley & Sons, Inc.

Cox, J. C. & Ross, S. A. (1976), 'The valuation of options for alternative stochastic processes', *Journal of Financial Economics* **3**, 145–166.

Derman, E. & Kani, I. (1994), 'Riding on a smile', *Risk* **7**(2), 32–39.

Derman, E., Kani, I. & Zou, J. (1996), 'The local volatility surface: Unlocking the information in index option prices', *Financial Analysts Journal* **(July-August)**, 25–36.

Duffie, D., Pan, J. & Singleton, K. (2000), 'Transform analysis and option pricing for affine jump-diffusions', *Econometrica* **68**, 1343–1376.

Dumas, B., Fleming, J. & Whaley, R. E. (1998), 'Implied volatility functions: Empirical tests', *Journal of Finance* **53**(6), 2059–2106.

Dupire, B. (1994), 'Pricing with a smile', *Risk* **7**(2), 229–263.

Feittelli, M. (2000), 'The minimal entropy martingale measure and the valuation problem in incomplete markets', *Mathematical Finance* **10**(1), 39–52.

Fleming, W. H. & Soner, H. M. (1993), *Controlled Markov Processes and Viscosity Solutions*, Springer-Verlag.

Fletcher, R. (1987), *Practical Methods of Optimization*, John Wiley & Sons.

Geman, H. & Madan, D. B. (2004), Pricing in incomplete markets: From abscence of good deals to acceptable risk, *in* G. Szegö", ed., 'Risk Measures for the 21st century', Wiley, pp. 451–474.

Hamida, S. B. & Cont, R. (2005), 'Recovering volatility from option prices by evolutionary optimization', *Journal of Computational Finance* **8**, 1–34.

Heston, S. L. (1993), 'A closed-form solution for options with stochastic volatility with applications to bond and currency options', *Review of Financial Studies* **6**, 327–343.

Hull, J. C. & White, A. (1987), 'The pricing of options on assets with stochastic volatilites', *Journal of Finance* **42**, 281–300.

Jackson, N., Süli, E. & Howison, S. (1999), 'Computation of deterministic volatility surfaces', *The Journal of Computational Finance* **2**(2), 5–32.

Merton, R. C. (1976), 'Option pricing when underlying stock returns are discontinuous', *Journal of Financial Economics* **3**, 125–144.

Nordén, L. (2003), 'Asymmetric option price distribution and bid-ask quotes: consequences for implied volatility smiles', *Journal of MultiNational Financial Management* **13**, 423–441.

Pooley, D. M., Forsyth, P. A. & Vetzal, K. R. (2003), 'Numerical convergence properties of option pricing pdes with uncertain volatility', *IMA. Journal of Numerical Analysis* **23**(2), 241–267.

Rouge, R. & Karoui, N. E. (2000), 'Pricing via utility maximization and entropy', *Mathematical Finance* **10**(2), 259–276.

Rubinstein, M. (1994), 'Implied binomial trees', *The Journal of Finance* **49**(3), 771–818.

A Tables

Two tables are presented in this appendix. Table 2 provides the assumed option prices under a CEV model. Table 3 described the S&P 500 market bid and ask prices on April 20, 1999 Andersen & Andreasen (2000).

Table 2: European option middle prices and associated implied volatilities of the CEV model example. The underlying price is assume to follow process (17). $S_0 = 100$, $r = 0.05$, $q = 0.01$.

Maturity (T_i)	Type	Strike (K_i)	Middle Price	Implied Vol
0.1	Call	105	0.4198	0.1464
	Call	100	2.0928	0.1500
	Put	95	0.3019	0.1539
0.25	Call	110	0.4234	0.1430
	Call	105	1.4047	0.1464
	Call	100	3.4924	0.1500
	Put	95	0.9001	0.1539
	Put	90	0.2388	0.1581
0.5	Call	115	0.5725	0.1399
	Call	110	1.3828	0.1431
	Call	105	2.8756	0.1465
	Call	100	5.2276	0.1501
	Put	95	1.6094	0.1539
	Put	90	0.6864	0.1581
	Put	85	0.2494	0.1626
0.75	Call	120	0.5962	0.1369
	Call	115	1.2606	0.1399
	Call	110	2.4069	0.1431
	Call	105	4.1817	0.1465
	Call	100	6.6687	0.1501
	Put	95	2.1077	0.1540
	Put	90	1.0802	0.1581
	Put	85	0.4992	0.1626
	Put	80	0.2067	0.1674
1.0	Call	125	0.5741	0.1341
	Call	120	1.1231	0.1369
	Call	115	2.0333	0.1400
	Call	110	3.4219	0.1431
	Call	105	5.3815	0.1465
	Call	100	7.9543	0.1502
	Put	95	2.4823	0.1540
	Put	90	1.4092	0.1582
	Put	85	0.7415	0.1626
	Put	80	0.3602	0.1674
	Put	75	0.1609	0.1727

Maturity	Type	80	85	90	95	100	105	110	115	120	130	140	150
0.08	Bid			28.05	25.29	22.17	18.95	15.50					
	Ask			30.13	26.44	23.03	20.10	19.57					
0.25	Bid		30.57	28.30	25.95	23.55	21.28	19.23	17.57	15.64			
	Ask		31.75	29.16	26.61	24.13	21.88	23.03	19.03	19.28			
0.50	Bid		29.70	27.78	25.96	24.22	22.56	20.98	19.65	18.58	16.22		
	Ask		30.50	28.44	26.52	24.74	23.06	21.52	20.32	19.52	19.04		
0.75	Bid	30.96	29.36	27.74	26.15	24.61	23.22	22.01	21.02	20.14	18.50	16.40	
	Ask	31.82	30.08	28.36	26.69	25.11	23.70	22.51	21.56	20.78	19.63	19.22	
1.00	Bid	30.60	29.28	27.92	26.53	25.12	23.73	22.43	21.27	20.19	18.27	16.48	12.67
	Ask	31.40	29.96	28.52	27.07	25.62	24.21	22.91	21.77	20.75	19.12	18.19	18.30

Table 3: Bid and Ask implied volatilities for the S&P500 index options on April 20, 1999. Strikes(K) are in percentage of S_0, maturities(T) are measured in years.